applied optics

Analysis of short wavelength infrared radiation during laser welding of plastics

J. Martan,* J. Tesař, M. Kučera, P. Honnerová, M. Benešová, and M. Honner

New Technologies Research Centre (NTC), University of West Bohemia, Univerzitni 8, 30100 Pilsen, Czech Republic
*Corresponding author: jmartan@ntc.zcu.cz

Received 18 January 2018; revised 27 March 2018; accepted 3 April 2018; posted 3 April 2018 (Doc. ID 319859); published 0 MONTH 0000

In this paper, a new measurement system and a new approach in calculation for infrared (IR) radiation investigation in quasi-simultaneous transmission laser welding of plastics are presented. The measurement system is based on a MW/SWIR (medium-wave/short-wave IR) camera and optical filters narrowing the spectral region to SWIR. The measured signals contain radiation from the melted zone in between the semitransparent and absorbing polymers, as well as radiation from the surface and interior of the semitransparent polymer. The new calculation approach was developed to distinguish between these signals. It is based on simplification of the process to two places with two temperatures (surface and molten interface) and knowledge of the spectral optical properties of the material, filters, and camera response. The results of measurement and calculation for three different optical filters and polyoxymethylene samples with two thicknesses are shown and discussed. Good agreement is obtained for the calculation variant using normal transmissivity of the semitransparent polymer. ©2018 Optical Society of America

OCIS codes: (110.6820) Thermal imaging; (110.3080) Infrared imaging; (140.3390) Laser materials processing; (160.4760) Optical properties; (160.5470) Polymers; (150.5495) Process monitoring and control.

https://doi.org/10.1364/AO.99.099999

1. INTRODUCTION

Laser welding of plastics is well known in industry (e.g., automotive, electronics, and medical) for its advantages of being fast, versatile, reliable, and nondisturbing to sensitive components of parts [1]. It is also a promising way to connect polymer composites with long-fiber reinforcements [2], which seems to be a substitute for steel in some lightweight constructions in the automotive and aerospace industries. For laser welding of polymer composites, process control is necessary to ensure reliable and tight joints. To enable process control by short-wave infrared (SWIR) radiation, good understanding of the process is necessary.

Quasi-simultaneous transmission laser welding technology is based on a continuous laser with a scan head and a clamping system pressing two plastic materials together. The upper plastic is semitransparent to enable transmission of laser radiation to the lower plastic, which absorbs the radiation and is heated and melted. The upper plastic is heated by conduction from the lower plastic and then also melted. The melting is done on the interface between plastics only, so the surface of the upper plastic is only partly heated by heat conduction. After melting of both components and cooling down, the weld is produced. The laser beam moves fast and many times on the welding contour during the process, which enables melting of the material on all places simultaneously. Under applied pressure, the melt flows out of the contact region, and the samples move toward each other. This movement is called a set path and is measured by contact distance measurement [1].

Understanding of the IR radiation sources (molten interface and upper semitransparent plastic) during welding and their spectral and spatial distribution enables deeper understanding of the welding process and increases the possibilities of its quality control in production. IR radiation emitted from the molten interface is partly transmitted through the upper semitransparent plastic and partly absorbed, depending on wavelength, thickness, and optionally, glass fiber content for composites. IR radiation from the upper plastic at a lower temperature (different temperatures at different depths) is emitted either near its surface without attenuation or emitted at bigger depth and partly transmitted through some part of it.

A long-wave infrared (LWIR, 7.5–14 μm) or medium-wave infrared (MWIR, 3.4–5 μm) camera was used to analyze the welding process and possibly can be used for quality monitoring or even process control in a production line [1,3–6]. For these wavelengths, the plastics used are usually opaque and surface temperature of the upper plastic is measured.

A pyrometer sensitive at SWIR (1.65–2.1 μm), combined with a scan head, was tested in laser transmission welding in contour and quasi-simultaneous configurations [7,8]. It was

found that SWIR wavelengths are interesting for quality control of laser transmission welding, because for these wavelengths the plastics used are semitransparent, and information about temperature at the molten interface can be obtained. However, only pyrometers have been used up to now. In the present study, we use an IR camera at SWIR wavelengths. Use of an IR camera is simpler for industrial application than using a pyrometer, because the combination of pyrometer with a scan head is complicated. Incorporation of the pyrometer into the scan head needs special optics to have the spot always in the same place [9]. An IR camera can easily also investigate other places besides the current laser position.

Laser welding of long-fiber reinforced thermoplastics was studied by an MWIR IR camera [2]. Surface temperatures were measured for different combinations of fiber orientation and laser movement trajectory. A study on long-fiber reinforced thermoplastics [9] with an SWIR pyrometer placed in different positions relative to the laser spot was done. The goal of development was a combined scan head for scanning laser and pyrometer independently, which would also enable control of laser power during welding for curved weld seams or sharp corners.

The optical properties of polypropylene (PP), polycarbonate (PC), and polyamide (PA) for laser transmission welding were investigated in [10] for pure polymers and for polymer composites with short glass fibers. The spectral dependence of scattering and absorbance was measured in a wavelength range from 0.25 to 2.5 μm from comparison of normal and hemispherical configuration signals. The scattering changed significantly with the wavelength, sample thickness, and glass fiber content.

Measurement by pyrometer (sensitive from 1.1 to 2.1 μm) in a pulsed mode of welding is proposed in [11] for overcoming saturation by laser radiation on the same wavelength (1.68 μm) during transmission welding without an absorber. Measurement is done in the laser-off period. The experimental method and numerical model for a semitransparent material temperature measurement/calculation using one channel IR pyrometer are described in [12].

Different numerical modeling techniques were applied for prediction of temperatures at different locations during the transmission laser welding process [3,6,13–16], but none of them was developed to predict IR radiation from the interface during the welding process.

The purpose of the present work is to understand more clearly the importance of different optical properties on the measurement of IR radiation and the importance of the sources of IR radiation (molten interface and surface) during quasi-simultaneous transmission laser welding of plastics. The goal of this work is to contribute to a future precise temperature measurement of the molten interface between plastics during welding and thus enable the process monitoring and control for reliable industrial production. The spectral transmissivity and reflectivity of polymers were measured in a wide range of IR wavelengths in normal and hemispherical configurations. The spectral emissivity was determined from them. It was introduced to evaluate its influence on the final signal. The transmissivity of optical filters was also measured. The new calculation method for the IR radiation signal is presented based on the knowledge of optical properties. The results of calculation are compared to the results of measurement for better understanding of the IR radiation emitted during the welding process.

2. EXPERIMENT

In this section, details of the experimental system for laser welding of plastics with an IR camera measurement system and optical properties measurements are presented.

A. Laser Welding with IR Camera Measurement

The laser welding system consisted of a 300 W fiber laser (IPG YLR-300/3000-QCW-MM-AC, wavelength 1070 nm) with a scan head (Scanlab intelliSCAN 20, objective EFL = 500 mm) and a pneumatic clamping system with distance and force measurement (Fig. 1). The welding process was quasi-simultaneous transmission laser welding with laser beam speed 5 $m \cdot s^{-1}$, spot diameter 1 mm, laser power 36 W (1 mm thick sample), and 63 W (2 mm thick), clamping force 87 N, and welding time 5.3 s. The different laser powers are necessary to produce good weldsto obtain approximately the same temperatures at the interface. For the thicker semitransparent polymer, the laser power has to be higher due to the lower transmissivity of this polymer. The samples were composed of semitransparent and absorbing polymers. The semitransparent polymer was 1 and 2 mm thick polyoxymethylene plate (POM-C nature) with size 25 mm × 50 mm. The absorbing polymer was 2 mm thick POM plate with carbon black (POM-C black) with size 25 mm × 40 mm. The melting temperature of both polymers was 165°C. The welding configuration was a T-joint. The laser beam was scanned on two parallel lines 1 mm apart to fill the 2 mm wide band of the absorbing polymer side. The length of the weld seam was 40 mm. The combination of the welding parameters (force, time, laser power) resulted in a set path (vertical sample movement during melting) bigger than 300 μm.

The IR measurement system consisted of two IR cameras (LWIR and MW/SWIR) and an optical filter in front of the MW/SWIR camera. The measurement system was mounted on the laser welding system (Fig. 1). The angle between the sample surface normal and the camera was 32° for the

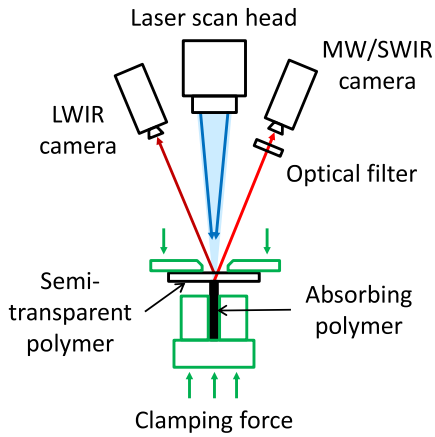

Fig. 1. Schematic representation of the experimental system. F1:1

LWIR camera and 22° for the MW/SWIR camera. The LWIR camera (FLIR A615), sensitive in the wavelength range from 7.5 to 14 μm, was used to measure the surface temperature of the semitransparent polymer. At these wavelengths, the POM polymer is opaque; the measured hemispherical transmissivity was about 0.1% for the 1 mm thick sample and smaller than 0.05% for the 2 mm thick sample. For the LWIR camera, a frame rate of 12.5 Hz and temperature range of −40°C to +150°C was used. The MW/SWIR camera (FLIR SC7650), sensitive in the wavelength range λ from 1.1 to 6.0 μm, was used to study IR radiation from the heated and melted interface during laser welding. This camera is cooled by a Stirling engine to very low temperatures and has high sensitivity and the possibility of measuring at high frequencies. Most of the measurements were done at frequency 870 Hz and integration time 1.2 ms. The camera was calibrated using a blackbody to investigate the dependency of the signal on integration time settings, and linear dependence was found. So, for other integration times used (0.2 and 0.6 ms), the signals were multiplied (by 6 and 2) to obtain the signal at integration time 1.2 ms. The lower and upper temperature limit (actual temperature range) depends on the integration time used for this camera. For 1.2 ms, it was 5°C to 50°C. The results are shown in a.u. (counts) because the measurement is done through the semitransparent polymer, and the values in temperature units (°C) are not valid.

Three different optical filters were used to limit the spectral sensitivity of the MW/SWIR camera to the SWIR range. This was done in order to enable measurement of IR radiation from the melted interface between the two polymers and decrease of radiation from the surface. The interface has a higher temperature compared to the surface, and so its radiation is shifted to shorter wavelengths. The filters SP-2600 and SP-3100 (Spectrogon) were shortpass filters with diameter 25.4 mm and thickness 0.5 mm. Their spectral transmissivity dependence is based on optical coatings. The filter WG12012-C (Thorlabs) was an N-BK7 glass optical window with diameter 50.8 mm and thickness 12 mm with an anti-reflection (AR) coating for wavelengths 1050–1700 nm. Its spectral transmissivity dependence is based mainly on the glass material and its thickness. The filter SP-2600 has significant transmission at about 4.5 μm wavelength, which was not known when it was acquired, but it is important for the camera signal.

B. Optical Properties Measurement

Optical properties of samples and filters were measured for use in the calculation of IR radiation for understanding of the measured IR radiation signal from the welding process. The spectral normal transmissivity τ (denoted later "normal transmissivity") of optical filters and POM samples were measured by an FTIR spectrometer with a normal transmission accessory. The spectral normal hemispherical transmissivity τ_H and reflectivity ρ_H (denoted later "hemispherical transmissivity and reflectivity") of POM samples were measured by an FTIR spectrometer (Nicolet 6700, incidence angle 12°) and UV-VIS-NIR dispersive spectrometer (Analytik Jena, Specord 210 BU, incidence angle 8°) using the integration sphere accessory and calibrated reference standards [17]. The hemispherical transmissivity and reflectivity values in the range from 1.1 to 1.5 μm were interpolated from the measurements on two spectrometers (FTIR and UV-VIS-NIR). Normal and hemispherical transmissivity values were measured for the calculation for comparison with measurement in order to understand which of these quantities is more relevant for the IR radiation measurement. The emissivity was measured in order to assess its influence in the resulting IR signal.

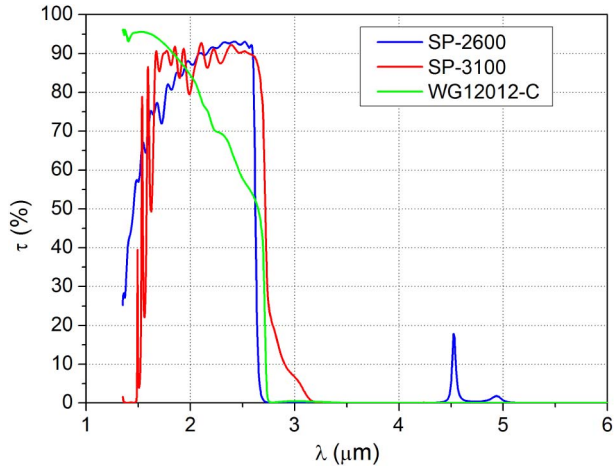

Fig. 2. Measured spectral normal transmissivity of the optical filters. F2:1 F2:2

The measured spectral normal transmissivity of the filters is shown in Fig. 2. The spectral optical properties of semitransparent samples are shown in Figs. 3 and 4. Hemispherical transmissivity and reflectivity account for light going in all directions after transmission or reflection by the sample. Normal transmissivity accounts only for light going in the same direction as the original light beam. As can be seen from Fig. 3, the POM material is significantly scattering light at short wavelengths of IR. The normal transmissivity is only 0.9% for the 1 mm thick sample at 2 μm wavelength, compared to 50% for hemispherical transmissivity. At middle-wave IR, the scattering is much lower. The normal transmissivity is 4.3% for the 1 mm thick sample at 4.6 μm wavelength, compared to 5.8% for hemispherical transmissivity.

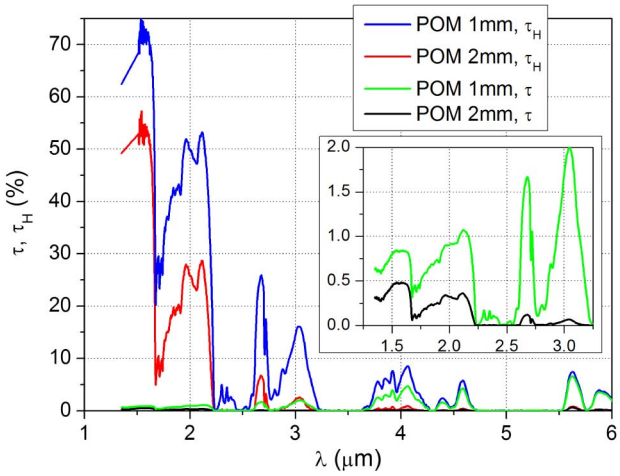

Fig. 3. Measured spectral normal and hemispherical transmissivity of natural (semitransparent) POM samples. F3:1 F3:2

Spectral emissivity ε was calculated from hemispherical transmissivity τ_H and hemispherical reflectivity ρ_H by Kirchhoff's law:

$$\varepsilon = 1 - \tau_H - \rho_H. \quad (1)$$

3. CALCULATION

The calculation approach for IR radiation is schematically represented in Fig. 5. The radiation from the laser welding process is simplified to radiation from two sources with two temperatures: upper surface of the semitransparent polymer and molten interface (upper surface of the absorbing polymer). The radiation from both sources goes to the MW/SWIR camera and produces together one measurement signal.

The interface between the two polymers is melted during the welding process. The melting temperature of the POM material was determined by differential scanning calorimetry (DSC) to 165°C. The degradation of the POM material starts at about 230°C [1]. The temperature of the molten interface T_{int} was set in the middle of the two temperatures to 200°C in the calculation. The thermal radiation emitted from the interface is described by Planck's law as spectral radiation intensity L_{int} (T_{int}, λ) at given wavelength λ and interface temperature T_{int}. The signal measured by the MW/SWIR camera from molten interface S_{int} is in the calculation given by the equation,

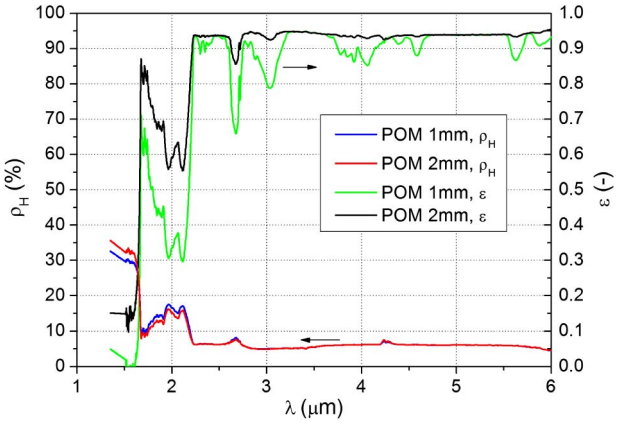

F4:1 F4:2 **Fig. 4.** Measured spectral hemispherical reflectivity and calculated emissivity of natural POM samples.

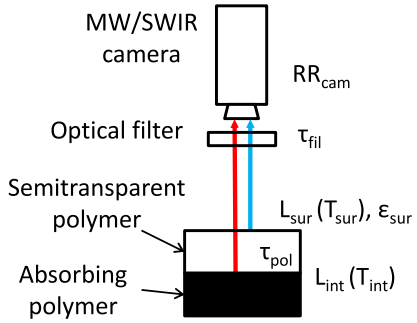

F5:1 F5:2 **Fig. 5.** Schematic representation of the SWIR measurement system for the purpose of calculation.

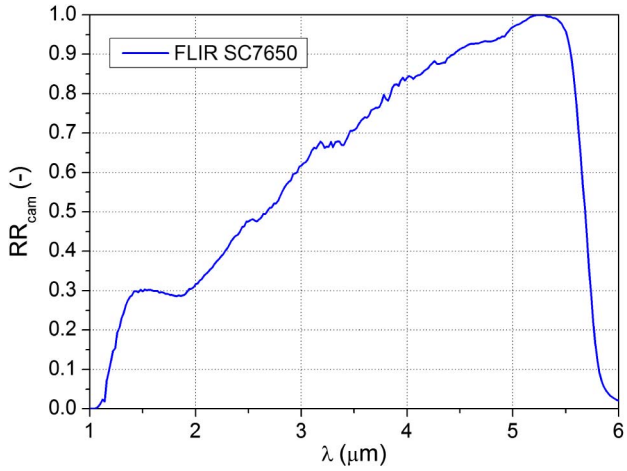

F6:1 **Fig. 6.** Relative spectral response of the MW/SWIR camera.

$$S_{\text{int}} = \int_{\lambda_1}^{\lambda_2} L_{\text{int}}(T_{\text{int}}, \lambda) \cdot \varepsilon_{\text{int}} \cdot \tau_{\text{pol}}(\lambda) \cdot \tau_{\text{fil}}(\lambda) \cdot RR_{\text{cam}}(\lambda) \cdot \mathrm{d}\lambda, \quad (2)$$

where ε_{int} is the spectral emissivity of the absorbing polymer sample, τ_{pol} is the spectral transmissivity of the semitransparent polymer sample, τ_{fil} is the spectral transmissivity of the optical filter, and RR_{cam} is the relative spectral response of the MW/SWIR camera. The relative response RR_{cam} of the MW/SWIR camera is shown in Fig. 6 (data obtained from camera supplier). The integration is done numerically with step 10 nm, and limits of integration are given by the spectral sensitivity of the camera and Planck's law signal: $\lambda_1 = 1.35$ μm and $\lambda_2 = 6.00$ μm. For the sample transmissivity τ_{pol}, either hemispherical or normal transmissivity is used in the calculation. The emissivity of the interface ε_{int} is assumed to be equal to 1, because the absorbing polymer is filled with carbon and has very high emissivity.

The thermal radiation emitted from the surface is described by Planck's law as spectral radiation intensity L_{sur} (T_{sur}, λ) at given wavelength λ and surface temperature T_{sur}. The signal measured by the MW/SWIR camera from surface S_{sur} is in the calculation given by the equation

$$\boldsymbol{S}_{\text{sur}} = \int_{\lambda_1}^{\lambda_2} \boldsymbol{L}_{\text{sur}}(\boldsymbol{T}_{\text{sur}}, \lambda) \cdot \varepsilon_{\text{sur}} \cdot \tau_{\text{fil}}(\lambda) \cdot RR_{\text{cam}}(\lambda) \cdot \mathrm{d}\lambda. \quad (3)$$

The emissivity of the semitransparent polymer ε_{sur} is, in the first stage, assumed to be equal to 1, and in the second stage, the spectral value calculated from the measured transmissivity and reflectivity of the sample is used.

The IR signal measured by the MW/SWIR camera during the welding process S_{IR} is in the calculation given by

$$S_{\text{IR}} = S_{\text{int}} + S_{\text{sur}}. \quad (4)$$

The calculation was done in two variants (see Table 1) in order to investigate the influence of optical properties on the agreement of the calculation with the experiment. In the first variant, the hemispherical transmissivity of the semitransparent polymer was used, and its emissivity was assumed to be equal to 1. In the second variant, normal transmissivity was used to

Table 1. Variants of Calculation of the IR Radiation Signal

Variant	Transmissivity of Semitransparent Sample	Emissivity of Semitransparent Sample
1	hemispherical	=1
2	normal	as measured

evaluate which type of transmissivity is valid for the IR camera temperature measurement, and the measured emissivity of the semitransparent polymer was introduced to evaluate its influence on the final signal. The transmissivity of the semitransparent polymer in the calculation affects only the interface signal, and the emissivity of semitransparent polymer affects only the surface signal. It is because τ_{pol} is present only in Eq. (2) and ε_{sur} is present only in Eq. (3).

4. RESULTS

In this section, the results of the measurement and calculation of IR radiation from the laser welding of plastics are presented.

A. Experimental Results

Examples of measured thermal images from the MW/SWIR camera are shown in Fig. 7. These images are without a filter for two thicknesses of the semitransparent sample (POM 1 and 2 mm) and with filters for the 1 mm thickness. For measurement without a filter, there is enough signal, and shorter integration times are used. For measurement with filters, the images are noisy even with longer integration time. The IR signal used for investigations was extracted as an average from signals of pixels in line L1 placed along the welding line in its center.

The signal distribution in distance from the welding line is different for different thicknesses [Figs. 7(a) and 7(b)]. For the thicker sample, the signal is more widely distributed. This can be caused by scattering of radiation inside the sample or by 3D heat conduction (compared to more 1D conduction in a thinner sample).

The IR signal evolutions over time measured without a filter are shown in Fig. 8 for two sample thicknesses. The signal rises more than linearly during laser heating; then, when the laser is switched off (5.3 s), it drops down rapidly by a certain step and then rises again. For the 1 mm thick sample, the signal in a few seconds after the laser switch-off stabilizes at maximum value. For the 2 mm thick sample, it rises for a much longer time. This is explained by the following hypothesis: The drop after the laser switch-off is the signal from the interface, where the temperature rapidly decreases when the laser is switched off. The rest of the signal is from the surface of the semitransparent material, where the temperature still rises due to heat conduction through the polymer. For lower thickness, the surface temperature stabilizes in a shorter time due to shorter distance from the heat source and lower heat capacity. The temperatures of the surface measured by the LWIR camera at the end of laser heating are 84°C and 45°C for 1 mm and 2 mm thickness.

The IR signal from measurements with different optical filters is shown in Figs. 9 and 10. The shape of the signal using the SP-2600 filter is very similar to the shape of the signal without a filter. This can be explained by the presence of a transmission peak at 4.5 μm wavelength for this filter, enabling radiation from the surface to be captured by the camera. The signals using filters SP-3100 and WG12012-C are different from the previously mentioned ones. After the end of laser

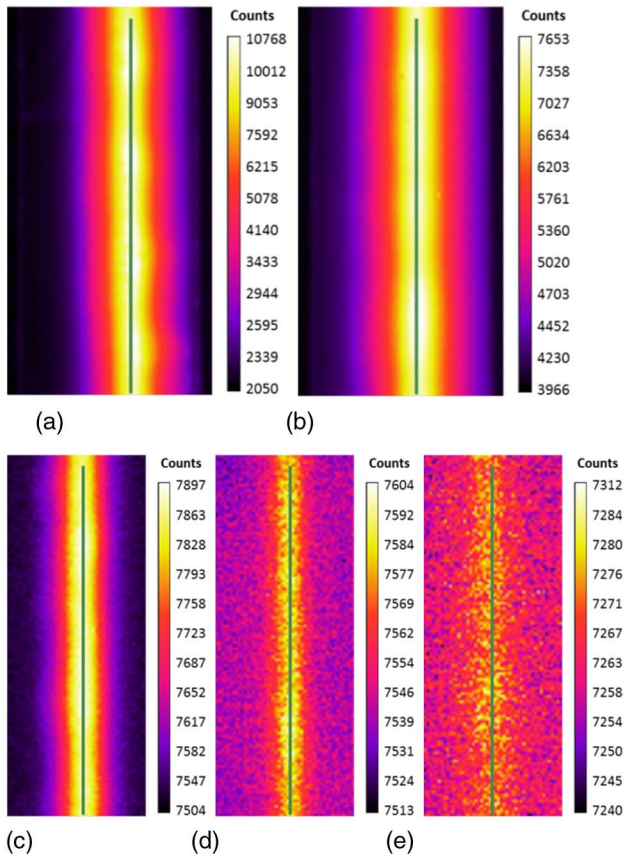

Fig. 7. Thermal images of the weld from the MW/SWIR camera at the end of laser heating.(a) Without filter, POM 1 mm, integration time IT = 0.2 ms; (b) without filter, POM 2 mm, IT = 0.6 ms; (c) filter SP-2600, POM 1 mm, IT = 1.2 ms; (d) filter SP-3100, POM 1 mm, IT = 1.2 ms; (e) filter WG12012-C, POM 1 mm, IT = 1.2 ms. The L1 line (green) is shown in the figures.

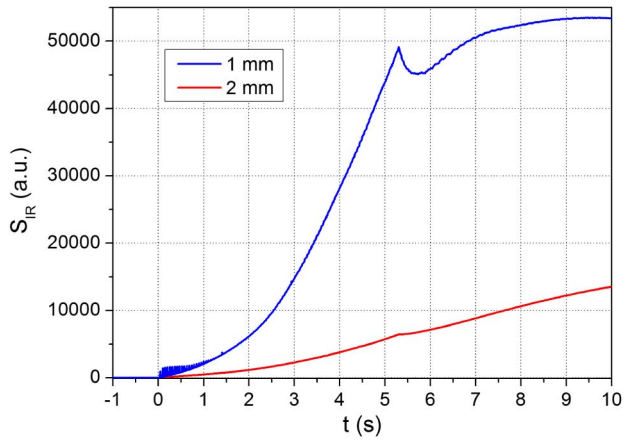

Fig. 8. Measured IR signal evolution over time from the MW/SWIR camera for two sample thicknesses.

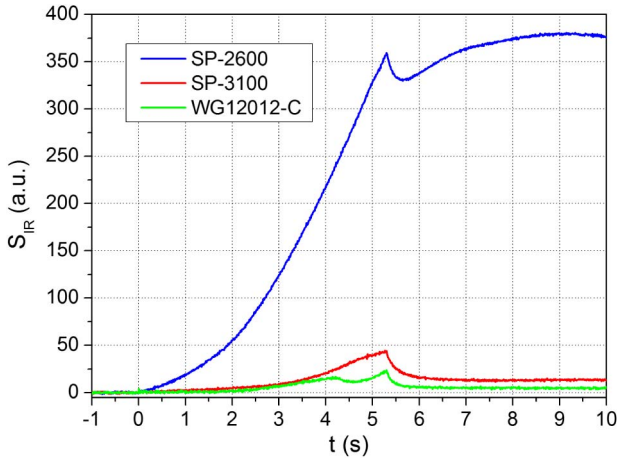

F9:1 F9:2 **Fig. 9.** Measured IR signal evolution over time from the MW/SWIR camera with different optical filters for sample thickness 1 mm.

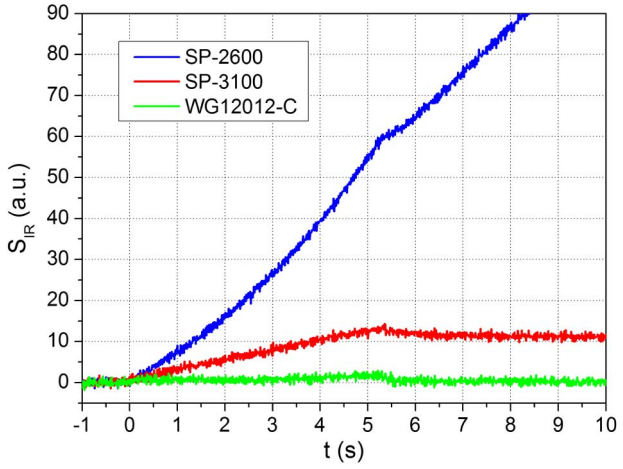

F10:1 F10:2 **Fig. 10.** Measured IR signal evolution over time from the MW/SWIR camera with different optical filters for sample thickness 2 mm.

heating, there is no increase of the signal for these cases. This means that the signal from the surface is sufficiently decreased to be able to clearly observe the signal from the interface. On the other hand, the signal from the interface is very low and noisy. The stable value of the signal several seconds after the laser switch-off is supposed to be the signal from the surface, and so the signal from the interface is assumed to be only the resting difference between the signal peak at the end of laser heating and the mentioned stable value. The IR signal curve for the WG12012-C filter (1 mm thick sample) has a different shape because the process was done with higher laser power (45 W), but the signal at the end of laser heating should be at a good level for comparison with other signals (during the melt flow, the temperature is relatively stable).

From the measured IR signal evolutions over time, the signal contributions from the interface and surface at the end of laser heating (5.3 s) were determined. They are shown in Table 2. The surface IR signal for the SP-3100 and WG12012-C filters

Table 2. Measured IR Signal from the Surface of the Semitransparent Polymer and the Interface between Two Polymers for Different Filters at the End of Laser Heating

	IR Signal (a.u.)			
	POM 1 mm		POM 2 mm	
Optical Filter	Interface	Surface	Interface	Surface
–	6863.1	42134.2	667.9	5777.2
SP 2600	40.1	316.9	4.2	55.7
SP 3100	29.8	13.4	2.4	11.3
WG12012-C	17.7	5.1	1.4	0.3

was determined as an average over time from 7 to 10 s. The interface signal for these filters was determined as the value at the end of laser heating minus the surface signal. For the measurement without a filter and with the SP-2600 filter, the surface value is not clear. A linear fit was done over time from 6 to 6.5 s for the 1 mm thick sample (6.5 to 7 s for the 2 mm thick sample), and its value at the end of the laser pulse (5.3 s) was said to be the surface signal. The interface signal for these measurements was determined as the value at the end of laser heating minus the surface signal. It can be seen that the signal from the interface is very low for the 2 mm sample thickness and when using optical filters. This can be due to significant scattering of the POM material and will be studied further in comparison with the calculation.

B. Calculation Results

The first step in the calculation is calculation of radiation given by Planck's law. Spectral radiation intensity calculated for the interface and surface temperatures used in the calculation are shown in Fig. 11. In the SWIR range (transmissivity of optical filters used, from 1.5 to 2.7 μm), the interface emits significantly more radiation than the surface at lower temperature.

Spectral results of the calculation are shown in Figs. 12–15. The curves include all variables in Eqs. (2) and (3) inside of integrals and are shown for surface and interface, each with the two variants (Table 1). In the results without a filter

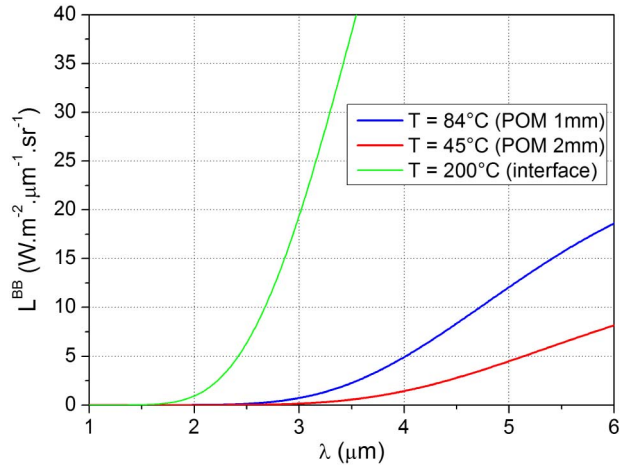

F11:1 F11:2 F11:3 **Fig. 11.** Spectral radiation intensity given by Planck's law for temperatures used in the calculation: temperatures of the interface and surfaces for two sample thicknesses.

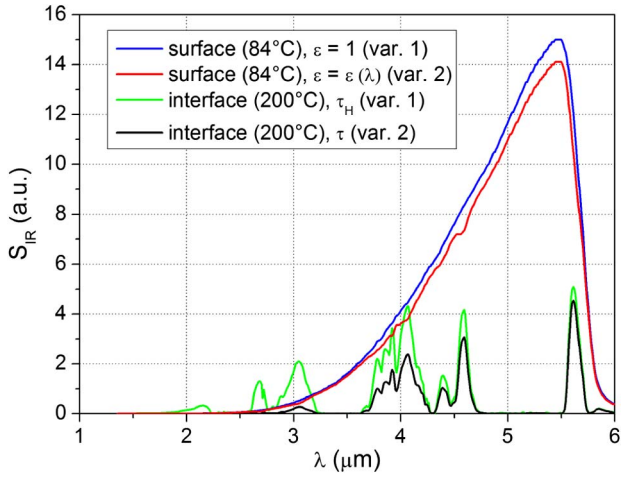

F12:1 F12:2 **Fig. 12.** Simulated spectral IR signal for measurement without a filter (different calculation variants).

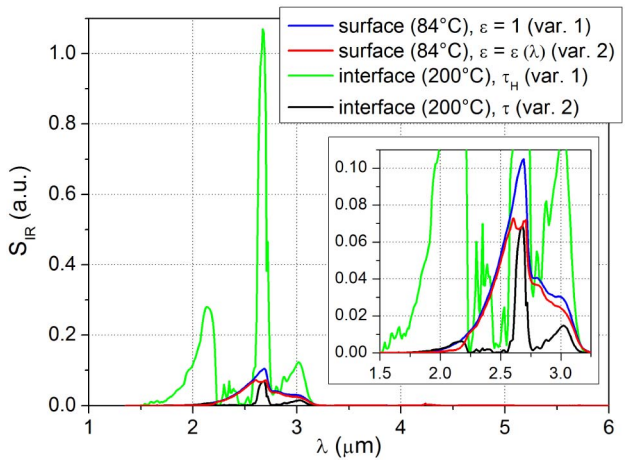

F14:1 F14:2 **Fig. 14.** Simulated spectral IR signal for measurement with the SP-3100 filter (different calculation variants).

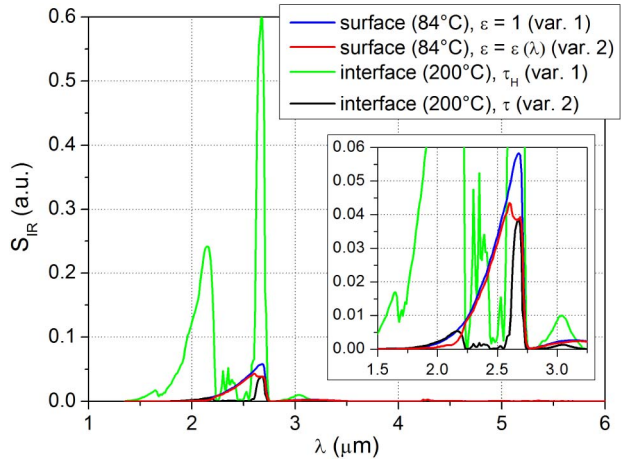

F15:1 F15:2 **Fig. 15.** Simulated spectral IR signal for measurement with the WG12012-C filter (different calculation variants).

and with filter SP-2600, there is a high amount of radiation from the surface, due to measurement also on longer wavelengths. For filters SP-3100 and WG12012-C, the radiation is restricted to shorter wavelengths up to 3.2 μm, as expected. The signal from the interface is present only in bands of transmissivity of the semitransparent polymer.

The influence of the type of transmissivity of the semitransparent polymer on the IR signal is very strong, mainly for the results with filters. The hemispherical transmissivity produces a high signal from the interface, much higher than the signal from the surface. For longer wavelengths, the influence of different transmissivity is lower. The material is scattering the radiation less there. The signal for normal transmissivity and with filters is significantly lower than the signal from the surface, mainly outside of the transmission bands.

The influence of the emissivity is relatively low. The region of low emissivity (<1.7 μm) is outside of the region of emission at surface temperature. The bands of medium emissivity (1.7–2.2 μm and 2.6–2.73 μm) influence the emission from the surface, but not dramatically. In other wavelengths, the emissivity is high, and so approximation of its value to 1 is appropriate at this level of simplification.

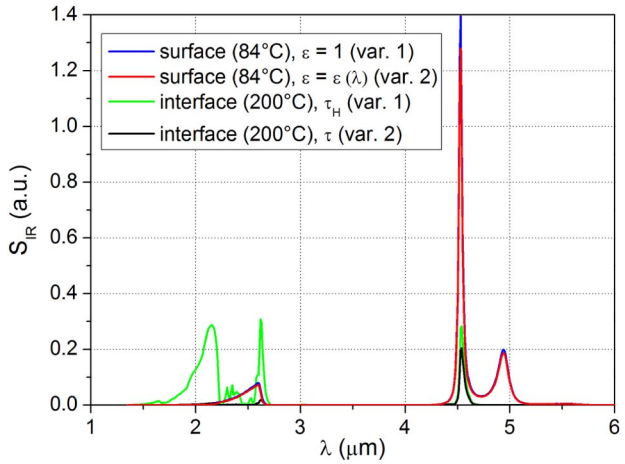

F13:1 F13:2 **Fig. 13.** Simulated spectral IR signal for measurement with the SP-2600 filter (different calculation variants).

The simulated IR signal after integration is shown in Table 3 for the two variants. The signal was multiplied by 10,000 in order to obtain regular numbers. This can simulate amplification of the signal by the internal preamplifier of the camera. The signal without a filter is very strong (100 times higher) compared to the signal with optical filters. This is in accordance with measurement. The detailed comparison is presented in the next section.

5. COMPARISON OF CALCULATION WITH MEASUREMENT

The comparison of measurement and calculation was done for the time of the end of laser heating (5.3 s). At this time, the biggest signal is from the MW/SWIR camera for the filters SP-3100 and WG12012-C, and the highest temperature is at the molten interface. The comparison can be done only by ratio in

Table 3. Simulated IR Signal of the MW/SWIR Camera Received from the Interface and Surface for Different Calculation Variants and Sample Thicknesses

Variant 1	IR Signal (a.u.)			
	POM 1 mm		POM 2 mm	
Optical Filter	Interface	Surface	Interface	Surface
-	31760.0	195180.0	2992.4	70436.0
SP 2600	1062.2	1293.4	339.2	409.2
SP 3100	1977.0	415.3	541.4	66.5
WG12012-C	1191.0	193.4	400.3	30.3
Variant 2	**IR signal (a.u.)**			
	POM 1 mm		POM 2 mm	
Optical Filter	Interface	Surface	Interface	Surface
–	17322.0	180350.0	774.7	66098.0
SP 2600	152.3	1182.2	8.4	383.3
SP 3100	109.2	347.2	8.6	61.1
WG12012-C	50.9	160.3	5.8	27.6

this case. Both measurement and calculation results are in arbitrary units. The ratio of calculation to measurement in each field of the table was selected for assessment of agreement of the results. The ratio was then divided by 4 for normalization to values around 1 for most fields. The normalized ratios are shown in Table 4. The colors indicate the level of agreement between measurement and calculation: green (the best) is from 1 to 1.5 or 1/1.5, yellow is to 2.5 or to 1/2.5, orange is to 5 or to 1/5 and red (the worst) is for bigger or smaller values.

From the ratios, it can be seen that variant 2 gives better agreement of calculation with measurement. The type of transmissivity significantly influences the agreement. Better agreement is given by normal transmissivity—mainly for using filters. For measurement without a filter, better results are with hemispherical transmissivity. The emissivity does not change the agreement significantly.

Table 4. Normalized Ratio of Calculation to Measurement Results of the IR Signal of the MW/SWIR Camera Received from the Interface and Surface for Different Calculation Variants and Sample Thicknesses

Variant 1	Ratio of IR Signals (–)			
	POM 1 mm		POM 2 mm	
Optical Filter	Interface	Surface	Interface	Surface
–	1.16	1.16	1.12	3.05
SP 2600	6.62	1.02	20.24	1.84
SP 3100	16.59	7.75	56.24	1.47
WG12012-C	16.87	9.53	73.42	25.07
Variant 2	**Ratio of IR signals (–)**			
	POM 1 mm		POM 2 mm	
Optical Filter	Interface	Surface	Interface	Surface
–	0.63	1.07	0.29	2.86
SP 2600	0.95	0.93	0.50	1.72
SP 3100	0.92	6.48	0.90	1.35
WG12012-C	0.72	7.90	1.06	22.83

Table 5. Normalized Ratio of Calculation to Measurement Results of the Whole IR Signal of the MW/SWIR Camera Received from the Interface and Surface Together for Different Calculation Variants and Sample Thicknesses

	Ratio of IR Signals (–)			
	Variant 1		Variant 2	
Optical Filter	POM 1 mm	POM 2 mm	POM 1 mm	POM 2 mm
–	0.93	2.28	0.81	2.08
SP 2600	1.32	2.50	0.75	1.31
SP 3100	11.08	8.87	2.11	1.02
WG12012-C	12.18	51.72	1.86	4.01

The biggest differences in variant 2 are for surface radiation with the WG12012-C filter for both thicknesses and with the SP-3100 filter with 1 mm thickness. The use of emissivity in the calculation decreased the difference, but only slightly.

Another comparison was done by comparing whole signals from measurement at the end of laser heating and the corresponding sum of the two signals from the calculation (interface + surface). This is shown in Table 5. In this case, the ratios were divided by 5 for normalization. Also in this case, variant 2 gives more consistent results than variant 1.

From the comparisons, it can be concluded that for measurement in SWIR wavelengths, the use of a normal value of transmissivity for the semitransparent polymer is more appropriate than the hemispherical value. Concerning selection of an appropriate optical filter, the best is use of filter SP-3100, because it does not transmit radiation from the surface (MWIR region), and it gives a bigger signal than filter WG12012-C.

In experiments with diffuse (scattering) materials in our laboratory, measurement of hemispherical transmissivity is usually performed, and so it was thought that it would be also appropriate for this case. For determination of emissivity of semitransparent (and diffuse) materials, the hemispherical transmissivity and reflectivity are essential. It was surprising that for the case of IR radiation emission measurement from the interface, the normal transmissivity is more appropriate.

For some materials, the difference between the normal and hemispherical transmissivity is negligible (e.g., PMMA), and there is no reason to distinguish between them. For POM 4 material, the difference is strong (strong scattering), and it was found to be important to choose the normal transmissivity.

The physical explanation is that the camera senses radiation in one direction (narrow solid angle), and so the normal (directional) transmissivity is more appropriate.

Concerning wavelength, from the optical properties measurement (Fig. 3), it can be seen that for the POM sample, the significant scattering is only at the SWIR wavelengths, and in the MWIR wavelengths there is low or no scattering. It may be that this could be the reason for better results of comparison between the calculation and measurement for measurement without a filter, where the major part of the signal is in the MWIR wavelengths (Fig. 12).

The most important uncertainty in the calculation was expected to be the temperature of the interface, but from the comparison of the calculation with measurement, the biggest difference is in the signal from the surface for use of the SP-3100 and WG12012-C filters. We are not able to explain the low signal from the surface in the measurement obtained with the filter WG12012-C. There can also be influences of experimental uncertainties, because the camera signal is very low and noisy for these cases.

The experimental IR measurement uncertainty of the system based on an MW/SWIR camera can be indicated by signal noise and an uncertainty of the camera. The noise of the MW/SWIR camera at the 1.2 ms integration time is ±0.8 a.u. (standard deviation, signal averaged over the line L1). The temperature measurement accuracy of the MW/SWIR camera (from datasheet) is ±1°C or ±1% of the measured value (the higher value is valid). From experimental data with the SP-2600 filter, it was deduced that ±1°C equals to ±156 a.u. This is significantly higher than most of the measured values, so the evaluated ratios can be significantly influenced by the accuracy of the camera. The relative manner of the measurement (difference to the signal corresponding to room conditions before laser welding) should minimize this influence.

Although the calculation is simple (e.g., not accounting for emission from the semitransparent sample interior, only from surface), the results are in reasonable correlation with measurements. The hypothesis regarding distinguishing signals from the surface and interface in measurement was confirmed. The calculation of the emission of IR radiation from different depths of the semitransparent sample is significantly more complicated due to different temperatures, transmissivities, and emissivities at different depths. This will be done in further research.

6. CONCLUSION

In the present work, a new measurement system and a new calculation of IR radiation were presented. It is a SWIR measurement system based on an MW/SWIR camera with an optical filter. The calculation is based on simplification of radiation sources to two places (interface and surface) and detailed knowledge of optical properties. The measurement system and calculation were applied to a quasi-simultaneous transmission laser welding of plastics.

In the measurement system, three different optical filters were used. During analysis using optical properties measurement, measurement of the welding process, and calculation, it was found that the most suitable is the SP-3100 filter, which has no transmission for higher wavelengths than 3.2 μm (as has filter SP-2600) and gives a higher signal from the interface than the WG12012-C filter.

In the calculation, the use of normal and hemispherical transmissivity of the semitransparent polymer and the use of constant emissivity and known measured emissivity of the semitransparent sample surface were compared. The calculation with normal transmissivity was in good agreement with the measurement for overall measurements, while hemispherical transmissivity gave good results only for measurement without a filter. This result was not expected, although the physical explanation is simple. The use of known emissivity improved the agreement of the calculation with measurement, but the influence was rather minor.

From the results, it can be concluded that the proposed measurement system with the SP-3100 filter is a suitable system for analysis of thermal processes during quasi-simultaneous laser welding of plastics. Its suitability for polymer composites and process control will be analyzed in further steps. The calculation presented has proven to be useful and gives good agreement with measurement, although it is relatively simple. The normal transmissivity has been shown to be a good value to be used for the presented measurement system, while the hemispherical transmissivity did not give good results for the presently studied POM polymer. In further research, the calculation will be used to predict IR signal evolution over time during and after the process, in combination with numerical modeling of temperatures in the samples.

Funding. Ministerstvo Školství, Mládeže a Tělovýchovy (MŠMT) (CZ.1.05/2.1.00/03.0088; LO1402); Bayerisches Staatsministerium für Wirtschaft und Medien, Energie und Technologie; Ministerstvo pro místní rozvoj České Republiky.

REFERENCES

1. R. Klein, *Laser Welding of Plastics* (Wiley-VCH, 2012).
2. V. Wippo, P. Jaeschke, M. Brueggmann, O. Suttmann, and L. Overmeyer, "Advanced laser transmission welding strategies for fibre reinforced thermoplastics," Phys. Procedia **56**, 1191–1197 (2014).
3. M. Speka, S. Matteıă, M. Pilloz, and M. Ilie, "The infrared thermography control of the laser welding of amorphous polymers," NDT&E Int. **41**, 178–183 (2008).
4. V. Wippo, K. Rettschlag, W. Surjoseputro, P. Jaeschke, and O. Suttmann, "Laser transmission welding of semi-interpenetrating polymer networks-composites," J. Laser Appl. **29**, 022407 (2017).
5. M. Ilie, J. C. Kneip, S. Matteï, A. Nichici, C. Roze, and T. Girasole, "Through-transmission laser welding of polymers—temperature field modeling and infrared investigation," Infrared Phys. Technol. **51**, 73–79 (2007).
6. L. S. Mayboudi, A. M. Birk, and G. Zak, "Infrared observations and finite element modeling of a laser transmission welding process," J. Laser Appl. **21**, 111–118 (2009).
7. V. Wippo, M. Devrient, M. Kern, P. Jaeschke, T. Frick, U. Stute, M. Schmidt, and H. Haferkamp, "Evaluation of a pyrometric-based temperature measuring process for the laser transmission welding," Phys. Procedia **39**, 128–136 (2012).
8. A. Schmailzl, S. Hierl, and M. Schmidt, "Gap-bridging during quasi-simultaneous laser transmission welding," Phys. Procedia **83**, 1073–1082 (2016).
9. H. Dittmar, V. Wippo, P. Jaeschke, H. Kriz, K. Delaey, O. Suttmann, and L. Overmeyer, "Temperature monitoring independent of laser-beam-position during laser transmission welding of fibre reinforced thermoplastics," in *Lasers in Manufacturing Conference*, Munich, Germany (2015), pp. 1–7.
10. C. Y. Wang, P. J. Bates, and G. Zak, "Optical properties characterization of thermoplastics used in laser transmission welding: scattering and absorbance," Adv. Mater. Res. **97–**101, 3836–3841 (2010).
11. V. Mamuschkin, A. Haeusler, C. Engelmann, A. Olowinsky, and H. Aehling, "Enabling pyrometry in absorber-free laser transmission welding through pulsed irradiation," J. Laser Appl. **29**, 022409 (2017).
12. T. Fu, J. Liu, and A. Zong, "Radiation temperature measurement method for semitransparent materials using one-channel infrared pyrometer," Appl. Opt. **53**, 6830–6839 (2014).
13. L. S. Mayboudi, A. M. Birk, G. Zak, and P. J. Bates, "A three-dimensional thermal finite element model of laser transmission welding for lap-joint," Int. J. Model. Simul. **29**, 149–155 (2009).

14. B. Acherjee, A. S. Kuar, S. Mitra, and D. Misra, "Modeling of laser transmission contour welding process using FEA and DoE," Opt. Laser Technol. **44**, 1281–1289 (2012).
15. S. K. Sooriyapiragasam and C. Hopmann, "Modeling of the heating process during the laser transmission welding of thermoplastics and calculation of the resulting stress distribution," Weld. World **60**, 777–791 (2016).
16. C. Hopmann and S. Kreimeier, "Modelling the heating process in simultaneous laser transmission welding of semicrystalline polymers," J. Polym. **2016**, 3824065 (2016).
17. P. Honnerová, J. Martan, Z. Veselý, and M. Honner, "Method for emissivity measurement of semitransparent coatings at ambient temperature," Sci. Rep. **7**, 1386 (2017).

Queries

1. AU: In the sentence beginning “For these wavelengths,” are my changes OK? Have I retained your meaning?

2. AU: In the sentence beginning “The results are shown in,” does “a.u.” stand for “atomic units” or “arbitrary units?” Please spell out.

3. AU: In the sentence beginning “The spectral normal transmissivity τ,” please spell out “FTIR”.

4. AU: In the sentence beginning “For some materials, the difference between the normal,” please spell out “PMMA.”

5. AU: The funding information for this article has been generated using the information you provided to OSA at the time of article submission. Please check it carefully. If any information needs to be corrected or added, please provide the full name of the funding organization/institution as provided in the CrossRef Open Funder Registry (http://www.crossref.org/fundingdata/registry.html).

ORCID Identifiers

The following ORCID identification numbers were supplied for the authors of this article. Please review carefully. If changes are required, or if you are adding IDs for authors that do not have them in this proof, please submit them with your corrections for the article.

- J. Martan https://orcid.org/0000-0002-5832-4425